Detection of Cardiac Arrhythmias using Electrocardiogram Signals

A THESIS SUBMITTED IN PARTIAL FULFILLMENT

OF THE REQUIREMENTS FOR THE DEGREE OF

Master of Technology

in

Signal and Image Processing

By

MANU THOMAS

Department of Electronics and Communication Engineering

National Institute of Technology, Rourkela

Odisha -769 008, INDIA

2014

Detection of Cardiac Arrhythmias using Electrocardiogram Signals

A THESIS SUBMITTED IN PARTIAL FULFILLMENT

OF THE REQUIREMENTS FOR THE DEGREE OF

Master of Technology

in

Signal and Image Processing

By

MANU THOMAS

Roll No: 212EC6196

UNDER THE GUIDANCE OF

Dr. SAMIT ARI

Department of Electronics and Communication Engineering

National Institute of Technology, Rourkela

Odisha 769 008, INDIA

2014

Dedicated to

My Parents

Declaration

I hereby declare that the work presented in the thesis entitled as "***Classification of Cardiac Arrhythmias using Electrocardiogram Signals***" is a bonafide record of the systematic research work done by me under the guidance of **Prof. Samit Ari**, Department of Electronics & Communication, National Institute of Technology, Rourkela, India and that no part thereof has been presented for the award of any other degree.

Manu Thomas
212EC6196

Department of Electronics and Communication Engineering

National Institute of Technology Rourkela

Rourkela-769008, Odisha, India.

CERTIFICATE

This is to certify that the work in the thesis entitled "**Classification of Cardiac Arrhythmias using Electrocardiogram Signals"** by Manu Thomas is a record of an original research work carried out by him during 2013 - 2014 under my supervision and guidance in partial fulfillment of the requirements for the award of the degree of Master of Technology with the specialization of Signal and Image Processing in the department of Electronics and Communication Engineering, National Institute of Technology Rourkela. Neither this thesis nor any part of it has been submitted for any degree or academic award elsewhere.

Place: NIT Rourkela

Date:

Dr. Samit Ari

Assistant Professor, ECE Department

NIT Rourkela, Odisha

Acknowledgments

I convey my earnest gratitude to my supervisor Prof. Samit Ari for his direction, motivation and support throughout my project work. I would also thank all the faculty members of the ECE department, NIT Rourkela for their guidance and help in completing my thesis work. I also extend my gratitude to Manab, Dipak and all the students of the pattern recognition lab for their help, support and cooperation throughout the end of the project. I wish to express sincere thanks to my classmates for their encouragement, motivation and the experiences that they shared with me.. I am particularly thankful to my parents who taught me the value of hard study and commitment. I would also appreciate their support in the choices that I have made in life. Finally, I humbly bow my head with utmost gratitude before the God Almighty who always showed me the path to go and without whom I could not have done any of these.

Manu Thomas
212EC6196

CONTENTS

ABSTRACT

ECG is an important non-invasive clinical tool for the diagnosis of heart diseases.The detection of cardiac arrhythmias is a challenging task since the small variations in ECG signals cannot be distinguished precisely by human eye. The objective of this work is to detect cardiac arrhythmias with highest detection accuracy. Cardiac arrhythmias are classified using discrete wavelet transform (DWT) and dual tree complex wavelet transform (DTCWT) technique. The DWT feature set comprises of statistical features extracted from the sub bands obtained after decomposition of QRS complex signals up to 5 scales whereas the DTCWT feature set comprises of wavelet coefficients extracted from the 4th and 5th scale decomposition of QRS complex signals. The two sets of features are appended individually by four other features (AC power, kurtosis, skewness and timing information) extracted from the QRS complex signal of each cardiac cycle. These feature sets are independently classified using a multi layered perceptron (MLP) neural network based on back propagation algorithm. In this work, five types of ECG beat (Normal (N), Paced (P), Right Bundle Branch Block (R), Left Bundle Branch Block (L) and Premature Ventricular Contraction (V)) are classified from the 48 files of MIT-BIH arrhythmia database. The experimental results indicate that the DTCWT technique classifies ECG beats with an overall sensitivity of 94.64% while DWT technique classifies with an overall sensitivity of 91.23%.

LIST OF FIGURES

LIST OF TABLES

LIST OF ABBREVIATIONS

ECG	Electrocardiogram
MIT-BIH	Massachusetts Institute of Technology - Beth Israel hospital
NSR	Normal Sinus Rhythm
PAC	Premature Atrial Contraction
L	Left bundle branch block
R	Right bundle branch block
V	Premature Ventricular Contraction
P	Paced beat
F	Fusion of Ventricular and Normal Beat
f	Fusion of Paced and Normal beat
DWT	Discrete Wavelet Transform
DTCWT	Dual Tree Complex Wavelet Transform
MLP-NN	Multilayer perceptron neural network

CHAPTER 1

INTRODUCTION

1.1 Electrocardiogram

The electrocardiogram (ECG) indicates the electrical activity of the human heart. It offers cardiologists with helpful information regarding the rhythm and functioning of the heart. Medical attention is required for patients with abnormal morphology and heart rate in ECG signals since these abnormal cardiac rhythms may lead to life threatening situations. ECG signals are acquired by placing electrodes across the thorax or chest of human body for a limited time and the electrical recordings are visualized using an external device. The electrodes pick the electrical signals generated by the polarization and depolarization of heart muscles [1]. The flat line (isoelectric line) indicates the absence of electrical activity while a deviation from the isoelectric line indicates the electrical action of heart muscles.

1.2 The human heart

The heart cells have small difference in the concentration of ions across the cell membrane at resting stage. The positive ion concentration is high in the outside membrane when compared to the inner membrane of heart cells resulting in resting potential of 90mV. The activation of heart cells causes high permeability of Na^+ ion, resulting in a change of polarity across the cell membrane (depolarization). The change in cell potential from negative to positive and back causes a voltage pulse called action potential [2]. The action potential leads to contraction of heart muscles. The depolarization and repolarization activity of heart cells are measured using ECG. Sino atrial (SA) node is considered as the pacemaker of the human heart because the bunch of cells around SA node causes fast depolarization of heart cells.

The human heart contains four chambers as shown in Fig. 1.1. The top left and right chambers corresponds to left and right atria whereas the bottom left chamber corresponds to left ventricle and bottom right chambers corresponds to right ventricles. The SA node is located inside the right atrium and the depolarization of heart cells in the SA node causes the left and right atria to contract almost simultaneously [3]. The atria and ventricles are interconnected with each other by atrio ventricular valve. A group of cells in the right atrium called atrio ventricular (AV) node conducts the depolarization of atria by bundle of conducting fibers (Bundle of His) to the ventricles. All part of ventricles are depolarized by purkinje fibers which are located in the muscle walls of ventricles. The polarization and depolarization activity of heart muscles causes the electrical current that moves across the body. The change in the electric current is maximum when one portion of heart is completely polarized while the other is completely depolarized. The summation of action potential from the heart is represented by the electrocardiogram signal. The contraction of two atria forces the blood to flow into ventricles. The two ventricles start contracting once the signal is conducted from the atria and the blood is pumped from ventricles through pulmonary and aortic arteries.

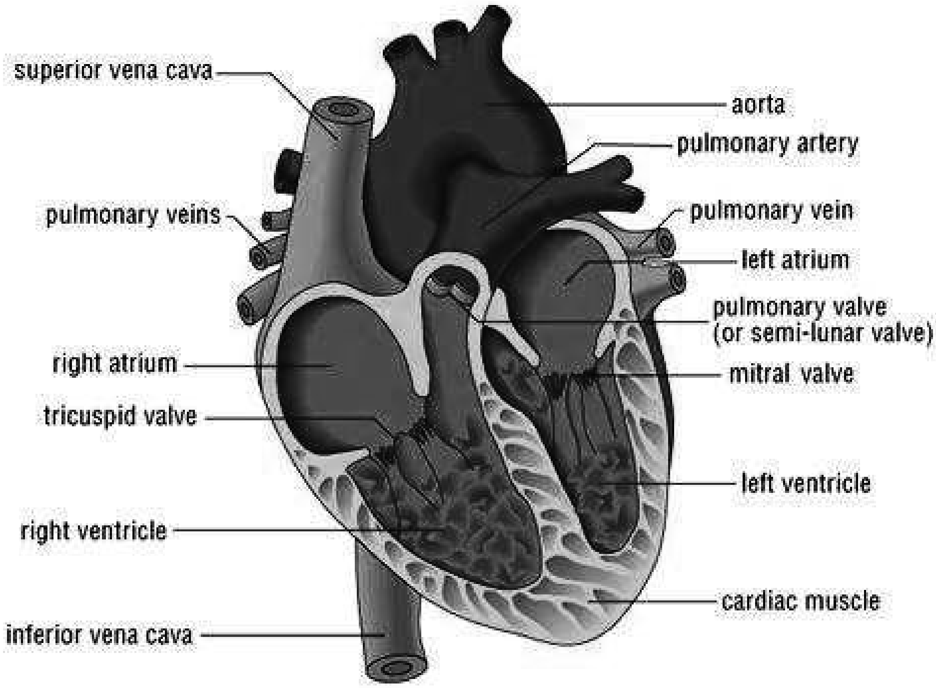

Figure 1.1: Anatomy of human heart

1.3 ECG Recording

The recording of ECG signals is performed by placing electrodes across the chest of the human body. The term lead refers to the electrical voltage difference between two electrodes. The most commonly used lead system for recording the ECG signals is 12-lead ECG system which includes three classes of leads [4].

- Bipolar leads – It refers to the lead I, II and III. The electrodes are connected to the right arm (RA), left arm (LA) and left leg (LL).
  (i) Lead I correspond to the voltage difference between the LA and RA.
  (ii) Lead II corresponds to the voltage difference between the LL and RA.
  (iii) Lead III corresponds to the voltage difference between the LL and LA.
- Augmented unipolar leads – It refers to the lead IV, V and VI as shown in Fig. 1.2. The positive electrode is placed at right arm for lead IV, left arm for lead V and left leg for lead VI while the negative electrode is placed at the centre of heart electric field which acts as the reference point. The leads under this category are:

(i) Augmented Vector Right (aVR) is the difference between the electrical potential of right arm and centre of heart electric field.

(ii) Augmented Vector Left (aVL) is the difference between the electrical potential of left arm and centre of heart electric field.

(iii)Augmented Vector Foot (aVF) is the difference between the electrical potential of left foot and centre of heart electric field.

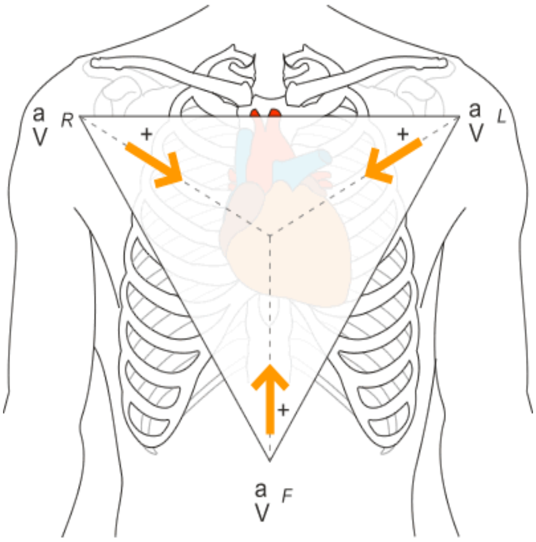

Figure 1.2: Augmented unipolar leads [5]

- Unipolar precordinal leads–It refers to the lead V1-V6. The leads are obtained by taking the difference between potential of electrodes placed on chest and centre of the heart electric field.

1.4 ECG waveforms

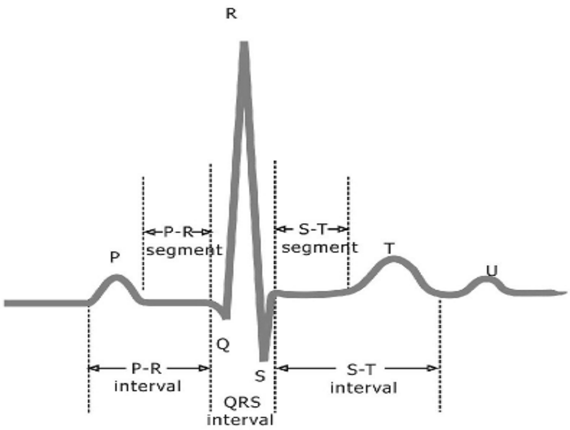

Figure 1.3: ECG signal representing one cardiac cycle [6]

Each cardiac cycle of ECG signal consist of a P, QRS, T and U wave as shown in Fig. 1.3.

- P wave: The first upward pulse from the isoelectric line followed by return to the isoelectric line corresponds to the P wave and it exists for duration of 0.04 sec. The depolarization activity of atria's causes the contraction of left and right atria resulting in P wave. [7]
- QRS complex wave: This signal results due to the depolarization activity of ventricles. The Q wave is a downward pulse which is followed by R wave with sharp positive peak. The R wave is followed by the S wave with a negative swing. The Q, R and S wave together constitute the QRS complex signal which indicates the time for the contraction of ventricles and it exist for duration of 80-120 msec [7].
- T wave: The QRS complex signal is followed by the T wave. It is an upward pulse which indicates the repolarisation of ventricles.
- U wave: The repolarisation activity of purkinji fibers is indicated by a small deflection following T wave called the U wave.
- PR segment: The P and QRS waves are connected by PR segment. In this duration of time the electrical impulse from AV node travels from atria to the ventricle. The PR segment represents a flat signal since there is no contraction of heart muscles occurring during that interval.
- ST segment: This segment interconnects the QRS and T wave. The ST segment represents the depolarization activity of ventricles. The duration of ST segment is approximately 80-120 msec.

1.5 Noises embedded in ECG signals

It is difficult for medical experts to analyse ECG signals embedded with noise. The noise removal technique is a challenging task due to spectral overlap between ECG signal and noise signal. The different types of noises that affect the ECG signals are:

1.5.1 Baseline wander

Baseline wander results in the movement of isometric line in upward and downward direction. It is caused due to the movement of electrodes connected across the chest during breathing or due to the movement of arm or leg. The variation in temperature and bias of the instrumentation amplifier circuit can also be a cause of baseline drift. It is a low frequency noise with a frequency range of 0 - 0.5Hz [8].

1.5.2 Power line interference

It occurs due to the poor grounding of ECG machines connected to the power supply [9]. The ECG machine picks up the ac signal of 50/60 Hz frequency and displays a thick looking ECG signal.

1.5.3 Electromyogram (EMG) interference

The electrical activity of muscles causes the contraction of muscles. The resulting signals are band limited Gaussian noise with a zero mean distribution. The EMG interference causes fast fluctuations which are faster than the ECG signals [4]. Its frequency range is 0-10 KHz and occurs for duration of 50msec [9].

1.6 ECG Arrhythmias

A normal sinus rhythm (NSR) represents an ECG signal with no cardiac disorder and has a heart rate of 60-100 beats per minute (BPM). A heart rate beyond 100 BPM indicates sinus tachycardia while a heart rate below 60 BPM indicates sinus bradycardia which affects the vital organs.

1.6.1 Sinus node arrhythmias

The SA node of the heart is responsible for this type of arrhythmias. The distinguishing feature of this type of arrhythmias is that the morphology of P wave of ECG signals remains normal. Sinus arrhythmia, Sinus bradycardia, and Sinus arrest are different type of arrhythmias which comes under the category of sinus node arrhythmias.

1.6.2 Atrial arrhythmias

These types of arrhythmias originate inside the atria but outside the SA node. The different types of atrial arrhythmias are:

- **Premature Atrial Contractions (PAC)**

  The P wave has abnormal morphology while the QRS and T wave have normal morphology. This problem arises due to the early firing of ectopic pacemaker before the SA node. Atrial tachycardia is characterized by the occurrence of PAC as triplet or more.

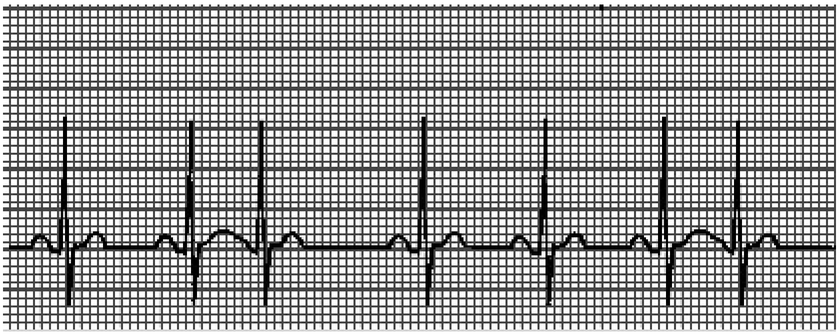

Figure 1.4: Premature atrial contraction

- **Atrial Tachycardia**

  This arrhythmia shows a heart rate of 160 to 240 BPM. The symptoms of atrial tachycardia are feeling of palpitations, nervousness and anxiety.

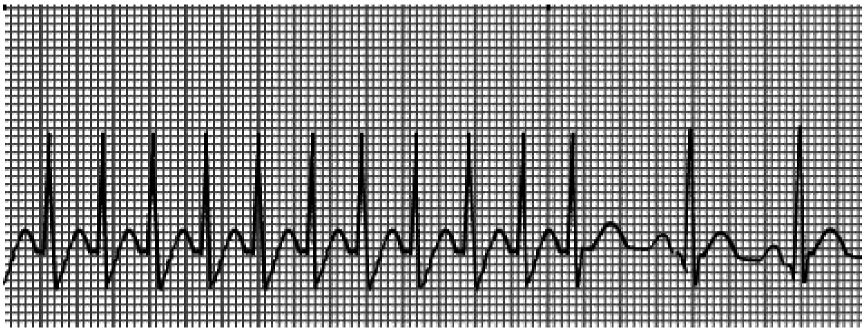

Figure 1.5: Atrial Tachycardia

- **Atrial Flutter**

  These types of arrhythmias are characterized by a very high heart rate (240-360 BPM). The P wave occurs at a fast rate and looks like a saw tooth waveform and hence it is called Flutter wave.

Figure 1.6: Atrial flutter

- **Atrial Fibrillation**

The atrial rate exceeds beyond 350 BPM and it occurs due to the uncoordinated stimulation of different portions of atria. A high atrial rate does not allow the ventricles to get completely filled with blood. Atrial fibrillation causes short bursts or chronic [1].

1.6.3 Junction Arrhythmia

These types of arrhythmias occur due to the firing of AV node or its bundles. The P wave has an abnormal morphology with opposite polarity when compared to the P waves of normal sinus rhythm due to the depolarization occurring from the AV node to the atria [1].

1.6.4 Ventricular Arrhythmia

This type of arrhythmias is characterized by wide QRS complex signal with bizarre shape. The impulse signal originates on ventricles and move to the remaining portion of heart.

- **Premature Ventricular contraction**
  The heart beat is triggered by the purkinje fibers in the ventricles resulting in the contraction of ventricles before the complete depolarization of atria. Lack of oxygen in cardiac muscles may cause PVC beats and they can occur anywhere in the ECG beat cycle.
- **Ventricular Tachycardia**
  The ventricular tachycardia is characterized by large and wide QRS complex signal when compared to the normal QRS complex signal. It is considered as a life threatening arrhythmias because of high heart rate (110 to 250 beats per minute) resulting in incomplete filling of ventricles.
- **Ventricular Fibrillation**
  Ventricular fibrillation occurs due to the firing of different ectopic pacemakers in a non-synchronized manner resulting in high ventricular rate. The wave appears to have saw tooth shape.

1.6.5 Bundle Branch Blocks

The bundle branch blocks results in myocardial infarction since there is a restriction in the movement of impulse signal from AV node to the entire conduction system. There are two types of bundle branch blocks (BBB). The right BBB prevents the impulse signal from AV node to depolarize the right ventricle while the left BBB prevents the depolarization of left ventricular muscles. These blocks results in myocardial infarction [1].

1.7 MIT-BIH ECG Database

The MIT institute in collaboration with Boston's Beth Israel Hospital (BIH) developed a standard database in 1980 for arrhythmia detection. This is the first standard database used by researchers to validate the performance of their proposed technique and compare their result with pre-existing algorithms. A total of 25 male patients with an age of 32 to 89 years and 22 female patients with an age of 23 to 89 years were chosen in order to include normal beat and common type of life threatening arrhythmias [10]. Each ECG record consists of two channel recordings. The first channel recording uses modified lead limb II (MLII) while the second channel recording commonly uses lead V1(V2, V4 or V5 for some patients). The database comprises of 48 recordings each containing 30 minutes segment of ECG selected from 24 hour recording of 47 different patients (200 and 201 ECG records are acquired from same patient) [8]. The first 23 (100-124) recordings correspond to the routine clinical recordings while the remaining recordings (200 – 234) contain the complex arrhythmias. The analog signals were sampled at a frequency of 360 Hz in order to use a notch filter with a notch frequency of 60 Hz for eliminating power line interference and band pass filtered at 0.1-100 Hz in order to avoid anti-aliasing and saturation in analog to digital conversion [10].

1.8 Wavelet transforms

In literature, numerous feature extraction techniques are applied to analyze and classify ECG beats such as the particle swarm optimization technique, principle component analysis, ECG morphological features in conjunction with timing information. Though these techniques have provided good classification results but the wavelet based techniques have outperformed when compared to the aforementioned techniques. The Fourier transform technique fails in analyzing non stationary signals due to its poor time frequency localization of the signal. The short time Fourier transform (STFT) analyses every spectral component with fixed window thereby providing fixed time and frequency resolution [11]. The uncertainty principle explains the inability to achieve high frequency and time resolution at same time instant. The wavelet transform (WT) technique helps in analyzing high frequency signal with high time resolution and low frequency signal with high frequency resolution by decomposing the input signal over scaled and shifted versions of a prototype wavelet [11]. The use of varying window size in wavelet transform helps in analyzing non stationary signal at multiple resolutions. In practical situations, the signals with high frequency component exist for short duration and low frequency component exist for long duration. The WT provides varying time-frequency window thereby analyzing high frequency component with narrow window and low frequency component with wide window [12]. The wavelet transform can be represented in continuous and discrete form.

1.8.1 Continuous wavelet transform

If $\psi(t)$ represents the mother or prototype wavelet such that $\psi(t) \in L^2(R)$, then a family of wavelet functions can be obtained by shifting and scaling $\psi(t)$ [13].

$$\psi_{r,s}(t) = \frac{1}{\sqrt{r}}\psi\left(\frac{t-s}{r}\right) \forall r, \mathrm{s} \in R\,(\,r > 0\,) \tag{1.1}$$

The parameter r and s corresponds to the scaling and translation factor respectively.

The chosen mother wavelet should satisfy the following admissibility condition

$$C_{\psi} = \int_{-\infty}^{\infty} \frac{|\Psi(w)|^2}{w} dw < \infty \tag{1.2}$$

Due to sufficient decay in $\Psi(w)$ the admissibility condition can be written as

$$\Psi(0) = \int_{-\infty}^{\infty} \psi(t) dt = 0 \tag{1.3}$$

Thus the equation 2.3 indicates that the wavelet function behaves as band pass function. The CWT of a signal $g(t)$ is defined as

$$\mathrm{CWT}_g(\mathrm{r,s}) = \int_{-\infty}^{\infty} g(t)\ \psi^*{}_{r,s}(t)\,\mathrm{dt} = \int_{-\infty}^{\infty} g(t)\frac{1}{\sqrt{r}}\psi\left(\frac{t-s}{r}\right) dt \tag{1.4}$$

The wavelet function $\psi_{r,s}(t)$ act as the filter bank impulse response. As the scaling parameter value increases the length of the window increases and hence the number of wavelet coefficient obtained in each stage decreases [14]. The wavelet coefficient $\mathrm{CWT}_g(\mathrm{r,s})$ indicates the correlation between the basis function and the input signal. The CWT is isometric in nature (it preserves energy) since CWT represents an orthonormal basis decomposition. The signal $g(t)$ can be reconstructed back from its wavelet coefficient as

$$g(t) = \frac{1}{C_\psi} \int_{-\infty}^{\infty} \int_{-\infty}^{\infty} \mathrm{CWT}_g(\mathrm{r}, \mathrm{s})\ \psi_{r,s}(t) \frac{drds}{r^2} \tag{1.5}$$

The CWT has high redundancy due to continuous values of the parameters (r & s) and it is difficult to implement in digital computer.

1.8.2 Discrete Wavelet Transform

The drawback of high redundancy in the case of CWT is overcome by discrete wavelet transform (DWT). It is achieved by using discrete values for scale and shift parameters. The discretization process is carried by replacing r by r_0^j and s by $kr_0^j s_0$, where $j,k \in Z$ [14]. Thus the family of wavelet functions after discretization process is given by

$$\psi_{\mathrm{l,m}}(t) = \frac{1}{\sqrt{r_0^l}} \psi\left(\frac{t - mr_0^j s_0}{r_0^j}\right) = r_0^{-l/2} \psi\left(r_0^{-l} t - ms_0\right) \tag{1.6}$$

The signal $g(t)$ can be represented as the sum of the wavelet function which is given by

$$g(t) = \sum_j \sum_k C_g(\mathrm{l,m})\ \psi_{\mathrm{l,m}}(t) \tag{1.7}$$

Where $C_g(\mathrm{l,m})$ represents the discrete wavelet coefficient. The most widely used discretization value for parameter r_0 and s_0 is given by 2 and 1 respectively [15]. The wavelet transform using these values is known as dyadic wavelet transform and the wavelet function obtained for discrete values of l and m is given by

$$\psi_{\mathrm{l,m}}(t) = 2^{-l/2} \psi\left(2^{-l} t - m\right) \tag{1.8}$$

The discrete wavelet coefficient is given by

$$C_g(\mathrm{l,m}) = \int_{-\infty}^{\infty} \psi_{\mathrm{l,m}}^*(t) g(t) dt = \langle \psi_{\mathrm{l,m}}(t), g(t) \rangle \tag{1.9}$$

The practical implementation of DWT comes from multi resolution analysis (MRA) and perfect reconstruction filter bank structure [16].

From MRA a scaling function (father wavelet) is introduced such that

$$\phi_{\mathrm{l,m}} = 2^{-l/2}\phi(2^{-l/2}t - m)\,;\ \mathrm{l,m} \in Z \text{ and} \int \phi(t)dt = 1 \tag{1.10}$$

Where $\phi_{l,m}$ is an orthonormal basis of the subspace V_j .If W_j is the orthonormal component of V_j then $W_j \perp V_j$ and $\psi_{\mathrm{l,m}} = 2^{-l/2}\psi(2^{-l/2}t - m)$. Here $\psi_{l,m}$ is the orthonormal basis of subspace W_j .

From equation2.7, the function $g(t)$ can be obtained from the scaling and wavelet function as

$$g(t) = \sum_{l=k_0}^{k_1}\sum_{m=-\infty}^{\infty} D_g(l,m)\phi_{l,\mathrm{m}}(t) + \sum_{l=k_0}^{k_1}\sum_{m=-\infty}^{\infty} C_g(l,m)\psi_{l,m}(t) \tag{1.11}$$

Where $D_g(l,m) = <\phi_{l,\mathrm{m}}(t), g(t)>$, $C_g(l,m) = <\psi_{l,m}(t), g(t)>$ and k_0 , k_1 are the finite lower and upper limit respectively such that $k_1 > k_0$. If $D_g(l,m)$ and $C_g(l,m)$ represents the scaling and wavelet coefficient obtained after the projection of signal $g(t)$ on to the subspace V_j and W_j respectively then the coefficient $D_g(l+1,m)$ and $C_g(l+1,\mathrm{m})$ can be obtained recursively from $D_g(\mathrm{l,m})$ and $C_g(\mathrm{l,m})$ as

$$D_g(\mathrm{l{+}1,m}) = \sum_n h_0(n-2m)D_g(\mathrm{l,m}) \tag{1.12}$$

$$C_g(\mathrm{l{+}1,m}) = \sum_n h_1(n-2m)C_g(\mathrm{l,m}) \tag{1.13}$$

Similarly the filter coefficient $C_g(\mathrm{l,m})$ can be derived from $D_g(\mathrm{l{+}1,m})$ and $C_g(\mathrm{l{+}1,m})$ as

$$C_g(\mathrm{l,m}) = \sum_n h_0(\mathrm{m}-2n)D_g(\mathrm{l{+}1,m}) + \sum_n h_1(\mathrm{m}-2n)C_g(\mathrm{l{+}1,m}) \tag{1.14}$$

The structure of filter bank up to 2 stages is shown in fig 2.2. The filter coefficient $D_g(\mathrm{l{+}1,m})$ is known as the approximation coefficient and $C_g(\mathrm{l{+}1,m})$ is known as the detail coefficient of $l+1$ scale [16]. The concatenation of all the coefficients from the last level of decomposition results in the DWT of the original signal.

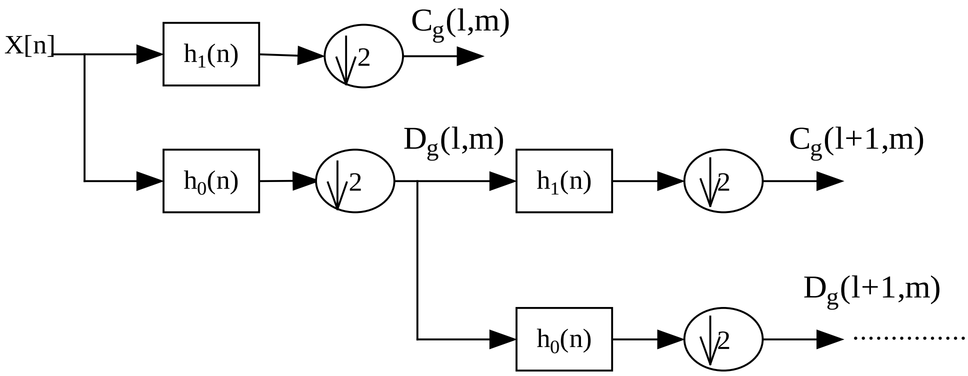

Figure 1.7: Filter bank implementation up to 2 stage DWT

1.8.3 Complex wavelet transform

The DWT technique is an excellent tool for analyzing non stationary signal, however they lack shift invariance property. The shift invariance property plays a key role in pattern recognition application such as ECG beat classification since a beat may be a shifted version of other. The lack of shift invariance results in large variation in the energy of the wavelet coefficients and hence the DWT transform fails to differentiate input pattern shifts. This occurs due to the down sampling operation at each stage. Hence there is a need for a transform which can provide approximate shift invariance with limited redundancy. The use of wavelet packets provides shift invariance at the cost of high redundancy. The complex wavelet transform provide approximate shift invariance with a limited redundancy of 2:1 for 1D signal [17]. The transform decomposes the input signal into real and imaginary components and compute the magnitude and phase information which helps in localizing the energy of wavelet basis functions. The analytic representation of signal gives a non-negative spectrum in the Fourier domain resulting in reduced bandwidth requirement and thereby overcoming the problem of aliasing which occurs among the frequencies of filter banks [17]. The concept of analytic representation is used among filter banks of DWT to give complex wavelet transform. The impulse response of two sets of real filters form a Hilbert transforms pair.

The DWT provides approximate shift invariance if each levels of the tree posses a sampling rate which is twice the initial sampling rate. This is performed by removing the down sampling by 2 operators in each stage resulting in two trees which are fully decimated. The technique works well up to level 1 beyond which this approach fails due to low sampling rate. A delay of half sample condition should be satisfied between the filters of two trees after level 1. A 2 band reconstruction block is shown in Fig. 1.19 which is designed to give perfect reconstruction from the analysis and synthesis filters. The average output from two trees gives an approximate shift invariant system. If the analysis and synthesis filter are designed with similar frequency response then the energy is preserved after the DTCWT transformation [18]. The reconstructed signal $\tilde{y}(t)$ using the coefficients follows perfect reconstruction and if the aliasing term is zero then the transform is shift invariant [17]. The transfer function E and F corresponds to the analytic filter bank while R and S represent the synthesis filter bank. As shown in Fig. 1.19.

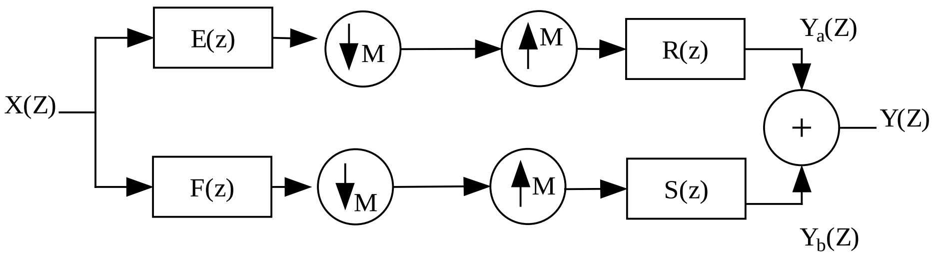

Figure 1.8: Two band Reconstruction Block

The odd/even type DTCWT filters suffers from various problems such as lack of perfect symmetry (the wavelet function of a particular level is not aligned to its scaling function), the two trees do not possess exact frequency response and the energy between signal and transform domains are not preserved due to the use of biorthogonal filters. These drawbacks are overcomed by using Q-shift dual tree. The filters used above level 1 are even in length and the group delay associated with them is $\frac{1}{4}$ samples (+q). A total difference in delay is $\frac{1}{2}$ sample (2q) due to the usage of the time reversed version of tree *a* filters in tree *b* filters resulting in a delay of 3q as shown in Fig. 1.20 [17]. The magnitude of complex wavelet function and its scaling functions are aligned to each other.

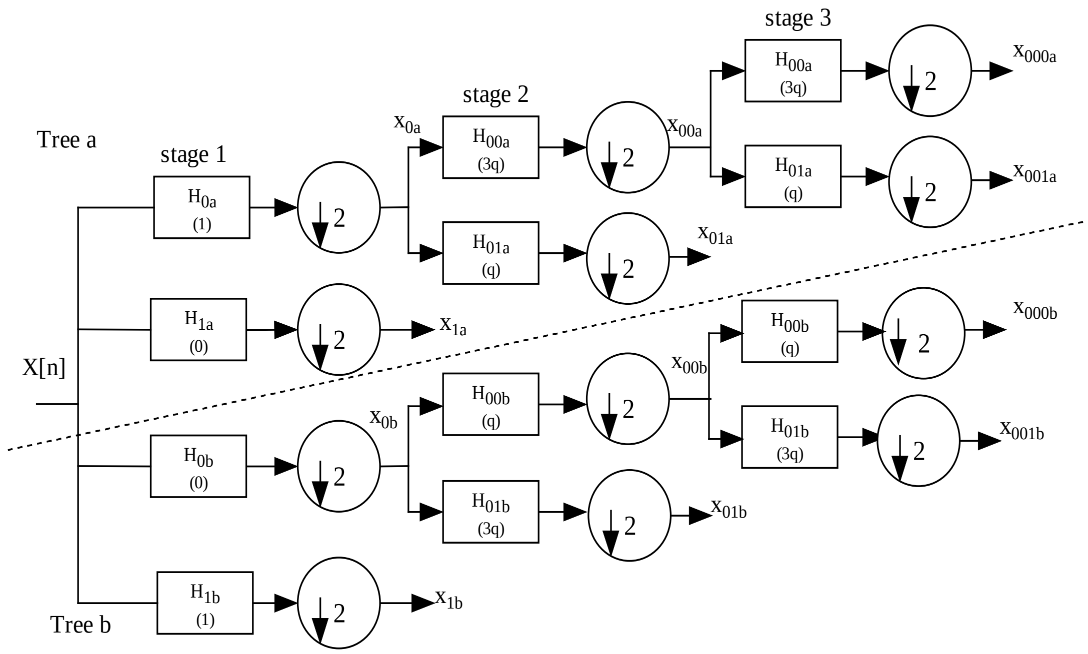

Figure 1.9: Q shift version of DTCWT

The remaining stages uses the same set of filters as mentioned above and the synthesis filter employs the time reversed version of the above mentioned filters. The filter coefficients used in each stage is described in [19].

1.9 Motivation

The electrocardiogram is widely used as a tool by cardiologists for determining the abnormalities of the human heart. An expert medical practitioner may fail to diagnose the heart abnormalities due to large variations in ECG signals resulting in life threatening situations. The detection of cardiac arrhythmias is a challenging task since the small variations in ECG signals cannot be distinguished precisely by human eye and the wave patterns may have to be analyzed for a long duration of time [20]. A doctor interprets an ECG signal based on its morphological shape and other parameters such as RR interval, PP interval, QT interval etc. The task of determining fiducial points and computation of parameter is a tedious job for doctors [21]. Hence there is a need for computer aided diagnosis system which consumes less computational time and achieves higher classification accuracy. Early detection of cardiac diseases using computer aided diagnosis system will result in the decline of high mortality rate among heart patients. In literature, numerous feature extraction techniques are applied to analyze and classify ECG beats. These techniques have shown high classification accuracy on small dataset of MIT-BIH database, hence the performance of these techniques on large dataset need to be explored for practical applications. In this project, a novel technique has been proposed for classifying five types of ECG beats, i.e. N, P, L, R and V beat using DTCWT technique and these features are independently classified using MLP based neural network.

1.10 Thesis outline

The chapter 1 gives a brief description about the basics of ECG signals, ECG recording leads, noises embedded in ECG signals, different type of cardiac arrhythmias, discrete wavelet transform and complex wavelet transform techniques. The chapter 2 explains the feature extraction steps using DWT and DTCWT technique. The experimental results obtained using MLP neural network are analyzed in the chapter 3. The conclusion of this report and future work is reported in chapter 4.

CHAPTER 2

FEATURE EXTRACTION TECHNIQUE USING DISCRETE WAVELET TRANSFORM AND DUAL TREE COMPLEX WAVELET TRANSFORM

2.1 Introduction

In literature, numerous feature extraction techniques are applied to analyze and classify ECG beats. In [22], Premature ventricular contraction (V) beats are classified from Normal (N) and other abnormal beats by using wavelet transform technique and timing information as feature. An overall accuracy of 95.16% is achieved by using ANN classifier. The ECG beats N, F, A, R, and f are classified using PSO and RBFNN in the literature [23]. The experimental results were limited over a small data set of MIT-BIH database. The ECG Arrhythmias detection using wavelet transform and probabilistic neural network gives an accuracy of 99.65% as reported in literature [24]. However the experimental results are limited to 23 ECG records of MIT-BIH database. In [25], the authors have used higher order statistics (HOS) of sub band components as feature and neural network based on back propagation algorithm as classifier. An accuracy of 96.34%is achieved using this technique. In [26] PCA is used as a tool for classifying five types of ECG beats (N, L, R, A and V). In the literature [27], the DTCWT features are used for EEG seizure detection. The seizure detection is performed on database selected from University of Bonn which gives 100% classification accuracy. ECG Arrhythmias detection using PCA and least square support vector machine were described in the literature [28] but the performance is evaluated on small dataset. In [29], the authors have used ECG morphology, heart beat intervals and RR intervals as feature and classifier model based on linear discriminants for classifying five types of ECG beats recommended by AAMI standard. In [30] the authors have used the statistical features from different parameters of the ECG signals for classifying four types of ECG beats. In [31], the DWT technique is used to analyze the effect of pulsed electromagnetic field on PPG, EEG and ECG signals. All the aforementioned techniques have shown significant performance only on small dataset of MIT-BIH database and hence these techniques may fail to classify ECG beats of large dataset.

In this work, a new technique is proposed for classifying ECG beats using DWT and DTCWT technique. The approximate shift invariance property of DTCWT makes the technique more useful in pattern recognition and signal analysis application [17]. Two sets of features were extracted using DWT and DTCWT technique. Each set of features were concatenated with four features extracted from the QRS complex of each cardiac cycle. In addition to the approximate shift invariance property, the DTCWT provides perfect reconstruction and limited redundancy which is independent of the number of decomposition levels (2^m for m-dimensional signal) and efficient computation (twice as simple DWT) [18]. The DWT is also an efficient tool for analyzing non stationary signals, however they lack shift invariant property i.e. the energy of the wavelet coefficient varies significantly as the input signal is shifted. The ECG beats of same patient may be of same type, however one may be slightly shifted version of the other. In such cases DTCWT classifies ECG beats efficiently than DWT technique. The variation in the energy of fourth scale detail coefficients obtained from the decomposition of two different L beats of #111 ECG records using DTCWT and DWT techniques are shown in Fig.2.5. The variation in energy of complex wavelet coefficient is very small when compared to the energy of DWT coefficients. The DTCWT uses two real wavelet filters which are Hilbert transform pair to each other. The combination of two such filters is termed as an analytic filter. The analytic filter gives a new structure equivalent to two standard DWT filter bank structures operating in parallel. The neural network based on back propagation training algorithm classifies ECG beats to appropriate classes. A comparative study is performed on classification performance of features extracted using DTCWT and DWT technique which is discussed in the next chapter. The experimental results indicate that DTCWT based features perform better than the DWT features for the 48 files of MIT-BIH database.

2.2 Proposed Method

The proposed technique consists of three main stages as shown in Fig. 2.2, (i) Pre-processing, (ii) Feature extraction and (iii) Classification. Amplitude normalization and filtering of ECG signals are performed in the pre-processing stage. The ECG signals are normalized such that the processed ECG signals have a mean of zero and standard deviation of one thereby reducing the variation in amplitude among each file. The embedded noises in ECG signals are removed by using a band pass filter operating at a frequency of 4-22 Hz. The pre-processed ECG signal is used for extracting significant features. The R peaks of ECG signals are located by using the annotation file of MIT-BIH database [8]. Various techniques for R peak detection can be found in literature [32-36]. The features extracted using DTCWT and DWT technique is feeded as input to an ANN classifier which maps the feature vectors to the respective class labels.

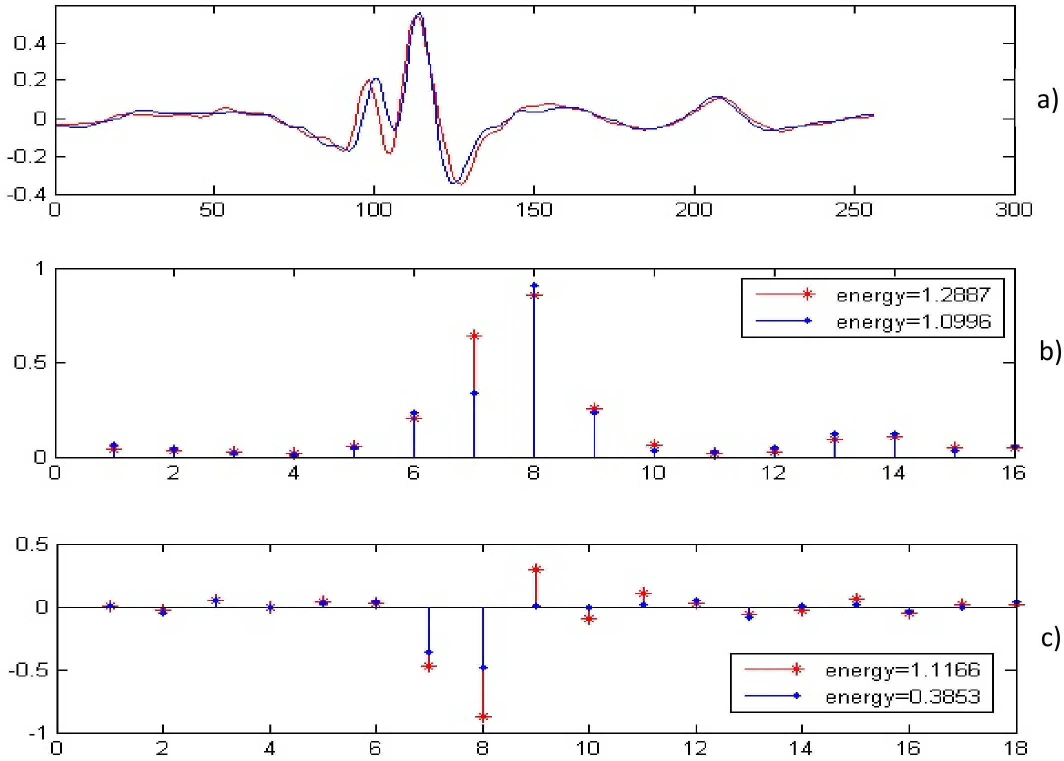

Figure 2.1: a) Two different L beats taken from #111 ECG record. b) Fourth scale detail coefficients of two L beats using DTCWT. c) Fourth scale detail coefficients of two L beats using DWT

2.3 Feature Extraction

The most important step in pattern classification problem is the choice of features from the given patterns. Feature extraction technique is a problem dependent task which varies for each application. The choice of feature extraction techniques is very important since a good classifier may fail to classify the beats, if the features selected are not proper [37]. It is the technique of extracting significant information from a signal thereby representing the signal in lower dimension. The feature extraction technique overcomes the problem of computational complexity and over fitting of the trained data. This report concentrates on the feature extraction technique based on DWT and DTCWT technique. The DTCWT features comprises of wavelet coefficients extracted from fourth and fifth scale of detail coefficients (D4 and D5) and DWT feature set consist of statistical features extracted from six sub bands i.e. from detail coefficients (D1, D2, D3, D4 and D5) and approximation coefficient (A5).

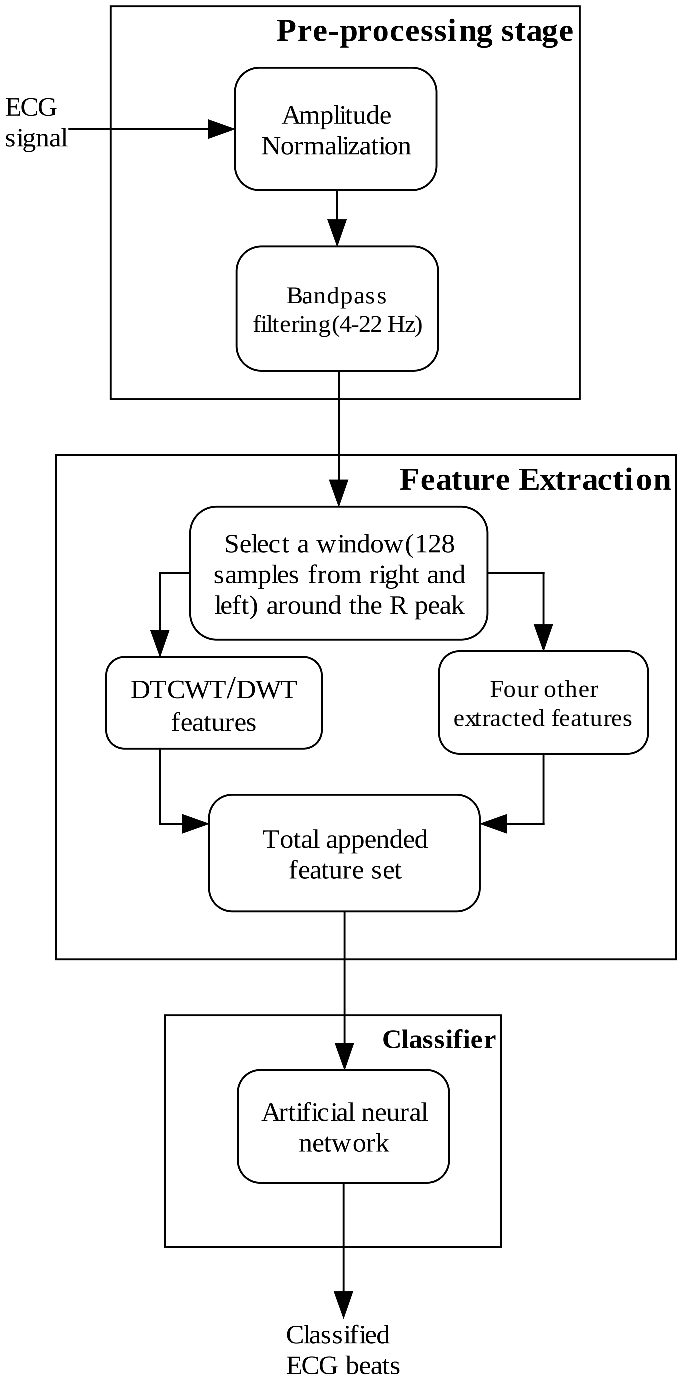

Figure 2.2: Methodology of proposed work

The two sets of features are appended individually by four other features (power, kurtosis, skewness and timing information) extracted from QRS complex of each cardiac cycle. The prototype wavelet used in DWT technique is daubechies wavelet of second order (Db2) due to its ability to detect the variations in ECG [31]. The DTCWT uses a specially designed Q shift filter as explained in the literature [17]. The DTCWT also provides good directional selectivity by suppressing the negative frequency components. Thus the DTCWT provides approximate shift invariance resulting in better performance when compared to the DWT technique. The numbers of decomposition levels completely depend on the maximum frequency content of the ECG signal [23]. The frequency ranges of sub bands after five scale decomposition using DWT or DTCWT technique is shown in Table 2.1. The predominant energy of the QRS complex signal lies in frequency range of 4-22 Hz hence the choice of 4th and 5th scale detail coefficient as feature using DTCWT technique is a good approach. The numbers of decomposition levels are limited to 5 beyond which baseline wandering become significant.

Table 2.1: Frequency ranges of the sub bands after five scale decomposition

sub band	Frequency range(Hz)
D1	90-180
D2	45-90
D3	22.5-45
D4	11.25-22.5
D5	5.63-11.25
A5	0-5.63

2.3.1 Extraction of feature set F1 using DWT

The feature extraction technique for feature set F1 can be summarized as:

(a) Extract the QRS complex signal by selecting a window of 256 samples around the R peak (select 128 samples from left and right of the R peak respectively).

(b) Decompose the QRS complex signal to five resolution scales by using 1D DWT technique.

(c) Select the decomposition levels corresponding to the detail coefficient sub band D1-D5 and approximation coefficient sub band A5. From each sub band four statistical parameters are computed i.e. maximum, minimum, mean and standard deviation of the wavelet coefficient.

2.3.2 Extraction of Feature set F2 using DTCWT

The feature extraction technique for feature set F2 can be summarized as mentioned below:

(a) Extract the QRS complex signal by selecting a window of 256 samples around the R-peak (select 128 samples from left and right of the R-peak respectively).

(b) Perform 1D DTCWT by decomposing the QRS complex signal up to 5 scales.

(c) Choose the 4th and 5th scale detail coefficients as features. The upper tree of complex wavelet transform gives the real part of 4th and 5th scale detail coefficients while the lower tree gives the imaginary part of 4th and 5th scale detail coefficients. The absolute value of the 4th and 5th scale detail coefficients are computed from real and imaginary coefficients.

(d) Perform 1D FFT on the selected features and take the logarithm of the Fourier spectrum.

2.3.3 Extraction of feature set F3

The feature sets F1 and F2 are appended by following four features (F3) extracted from QRS complex of each cardiac cycle. Let $x(n)$ represents the QRS complex signal.

(1) AC power: It indicates the total power content of the QRS complex signal

$$p = E\ [x^2(n)] \tag{2.1}$$

(2) Kurtosis: It indicates the peakedness of the QRS complex signal or it can be defined as a descriptor of the shape to the corresponding QRS complex signal.

$$kurt = \frac{E[(x-\mu)^4]}{\sigma^4} \tag{2.2}$$

(3) Skewness: It is a measure of the symmetry of the distribution of the signal and it also indicates whether the deviation from mean is positive or negative.

$$skew = \frac{E[(x-\mu)^3]}{\sigma^3} \tag{2.3}$$

(4) Timing information: It is given by R-R interval ratio which indicates the deviation from constant beat rate.

$$IR_i = \frac{T_i - T_{i-1}}{T_{i+1} - T_i} \tag{2.4}$$

Where T_i indicates the time of occurrence of R peak for the ith beat. The timing information differentiate the normal beat ($IR_i \cong 1$) from PVC beat ($IR_i < 1$)[22].

The feature sets used for classification using ANN can be summarized as:

FS1: Feature set F3 appended with feature set F1.

FS2: Feature set F3 appended with feature set F2.

The sets of features FS1 and FS2 are independently classified using artificial neural network. The extracted features set FS1 and FS2 are shown in Fig. 2.3 and 2.4 respectively.

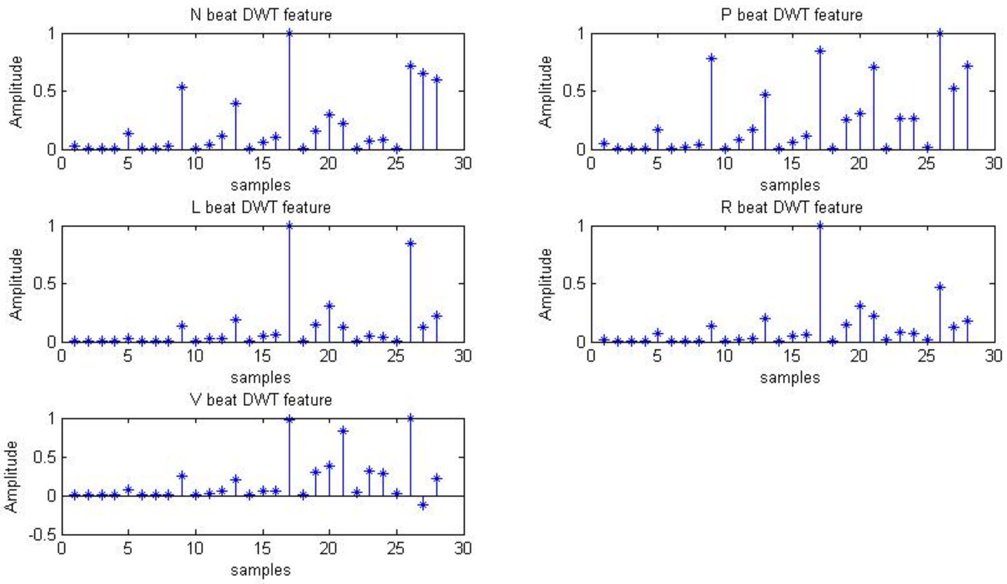

Figure 2.3: Extracted feature set FS1

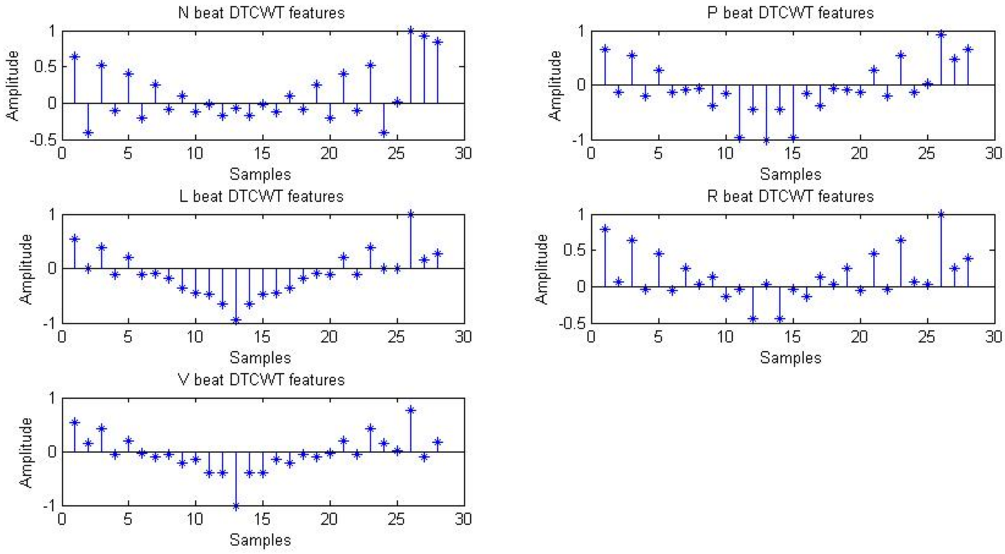

Figure 2.4: Extracted feature set FS2

2.4 Conclusion

A new technique for detecting cardiac arrhythmias is proposed using DTCWT technique. Two sets of features were extracted using DWT and DTCWT technique from 48 files of MIT-BIH database. Each set of features were appended by 4 other features (AC power, kurtosis, skewness and timing information) extracted from QRS complex of each cardiac cycle. The annotation file from MIT- BIH database is used for locating the positions of R-peaks. A total of 28 features represents one cardiac cycle. The classification performances of these features are discussed in chapter 3.

CHAPTER 3

CLASSIFICATION OF FEATURE SETS USING ARTIFICIAL NEURAL NETWORK

3.1 Introduction

In recent years neural network has been used as a tool for classification problems in many fields. The feed forward network architecture such as MLP, RBF network is commonly used in pattern recognition problems. The use of multiple layers in network architecture can solve complex mapping function problems. The patterns are given as input to the input layer which propagates in the forward direction from one layer to another layer. The MLP networks are trained by back propagation algorithm which employs supervised learning technique [39]. A well-known error correction algorithm used in MLP network is the least mean square (LMS) algorithm. The MLP network consists of two passes in the network. In the forward pass, the input patterns are applied to the input neurons and the signal propagates in the forward direction resulting in a group of outputs (actual response). The difference between the actual output and desired output gives the error signal [40]. In the backward pass, the error correction rule will determine the synaptic weights and the error signal propagates in the direction opposite to the synaptic weight connection. The weights are modified so that the actual output approaches the desired output.

3.2 MLP network architecture

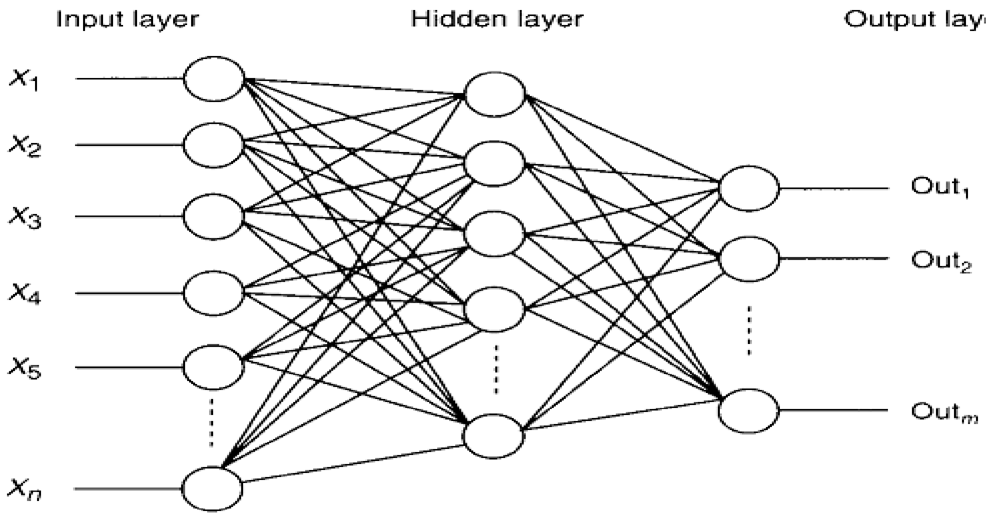

Figure 3.1: A three layered MLP network

The three important characteristics of a MLP network are:

1) An MLP network uses a nonlinear smooth activation function (differentiable at any point) which is superior to the hard limiter activation function [41].

2) The network consists of more than one hidden layers. The hidden neurons help to learn difficult problems by extracting significant information from input data.
3) The network has high connectivity.

The Fig. 3.1 represents a 3 layered MLP network. The MLP network contains two types of signals (Functional signal and Error signal).The functional signal is the input signal which propagates in the forward direction and emerges at the output of the network. The output signal is considered as the function of the input signal and corresponding weights. The error signal generated at the output propagates in the backward direction [42]. The hidden or output neuron performs two important tasks. They determine the output of a neuron which is the combination of nonlinear function of input and synaptic weight of that neuron. They also determine the gradient vector required for the synaptic weight updation during backward pass. If $y_j(n)$ indicates the output response of j^{th} neuron and $d_j(n)$ represents the desired response of j^{th} neuron then the error signal $e_j(n)$ is given by

$$e_j(n) = d_j(n) - y_j(n) \tag{3.1}$$

The weight updating equation is given by

$$w_{ji}(n+1) = w_{ji}(n) + \eta\delta_j(n)y_i(n) \tag{3.2}$$

Where η corresponds to learning rate parameter, $\delta_j(n)$ refers to the local gradient function and $y_i(n)$ corresponds to the input of j^{th} neuron for n^{th} iteration. If neuron *j* is considered as the output neuron then

$$\delta_j(n) = e_j(n)\phi^{'}(v_j(n)) \tag{3.3}$$

Where ϕ is the activation function and $v_j(n) = \sum_{i=0}^{m} w_{ji}(n)y_i(n)$

If neuron j is considered as the hidden neuron and neuron k as the output neuron then

$$\delta_j(n) = \phi^{'}(v_j(n))\sum_k \delta_k(n)w_{kj}(n) \tag{3.4}$$

Though back propagation algorithm is considered as an efficient computation technique but it doesn’t ensures optimal solution for all complex problems.

3.3 Performance matrix

Classification performance is evaluated using four common parameters as described in literature [37]. The parameter TP indicates true positive which comprises of set of beats belonging to the true class while the parameter TN indicates true negative which contains the set of beats which do not belongs to the true class and are correctly rejected. The set of real events which are classified as non-real events corresponds to false negative (FN) whereas the set of non-real events which are classified as real events is referred as false positive (FP).

(i) Accuracy (A_c): It indicates the overall performance of the system compared to all the ECG beats. It is measured by taking the ratio between the correctly classified beat to the total number of ECG beats.

$$A_c(\%) = \frac{TP + TN}{TP + TN + FP + FN} \times 100 \tag{3.5}$$

(i) Sensitivity (S_e): It is the ratio between the correctly classified ECG beats of a particular class to the total beats of that particular class.

$$S_e(\%) = \frac{TP}{TP + FN} \times 100 \tag{3.6}$$

(ii) Specificity (S_p): It is the measure of the ability of the classifier to reject the non-events.

$$S_p(\%) = \frac{TN}{TN + FP} \times 100 \tag{3.7}$$

(iii) Positive predictivity (P_p): It is the fraction of real events among the detected events.

$$P_p(\%) = \frac{TP}{TP + FP} \times 100 \tag{3.8}$$

3.4 Classification performance

The neural network used in our experimental study is a 3 layered, feed forward network, which employs the back propagation training algorithm with adaptive learning rate [43]. The MLP network is driven independently by two sets of features (FS1 and FS2). The size of input layer depends on the size of feature vector, and the number of classes determines the size of output layer. Hence, there will be 28 neurons in the input layer for feature set FS1 and FS2. The output layer employs 5 neurons. The hidden layer consist of

43 neuron, which is chosen empirically based on experimental results. The back propagation algorithm minimizes the average square error between the actual output and the desired output [44]. The activation function used is tan sigmoid function. Initially, the learning rate parameter is set to 0.5.

The MLP network is trained by using 48 files of MIT-BIH arrhythmia database. The first 3 minutes of each ECG record trains the network. The weights obtained after training the network is used for testing the remaining 27 minutes of each ECG record. The total number of ECG beats used for training and testing is shown in Table 3.1.

Table 3.1: ECG beats used for training and testing

CLASS	TRAINING BEAT	TESTING BEAT
N	7712	67268
P	654	6366
L	866	7347
R	758	6493
V	685	6420
	10675	93894

The Table 3.2 and 3.3 shows the confusion matrix and performance matrix for the feature sets FS1 respectively.

Table 3.2: Confusion matrix of FS1

CONFUSION MATRIX OF FS1 [DWT FEATURE]					
Class	N	P	L	R	V
N	64543	724	1240	598	163
P	310	5913	17	0	126
L	1128	256	5601	19	343
R	1941	2	95	4446	9
V	613	366	195	88	5158

Table 3.3: Performance matrix of FS1

PERFORMANCE MATRIX OF FS1 [DWT FEATURE]				
Class	Ac(%)	Se(%)	Sp(%)	Pp(%)
N	92.85	95.95	85.01	94.18
P	98.08	92.88	98.46	81.44
L	96.49	76.24	92.24	78.36
R	97.07	68.47	99.29	86.31
V	97.97	80.34	99.27	88.95
overall sensitivity = 91.23%				

The Table 3.4 and 3.5 shows the confusion matrix and performance matrix for the feature sets FS2 respectively.

Table 3.4: Confusion matrix of feature set FS2

CONFUSION MATRIX OF FS2 [DTCWT FEATURE]					
Class	N	P	L	R	V
N	65968	134	625	207	334
P	68	6225	35	14	24
L	981	157	5925	11	273
R	1024	2	114	5341	12
V	639	144	169	59	5409

Table 3.5: Performance matrix of feature set FS2

PERFORMANCE MATRIX OF FS2 [DTCWT FEATURE]				
Class	Ac(%)	Se(%)	Sp(%)	Pp(%)
N	95.73	98.07	89.81	96.05
P	99.38	97.79	99.50	93.44
L	97.48	80.65	92.57	86.27
R	98.46	82.26	99.73	94.83
V	98.24	84.25	99.26	89.38
overall sensitivity = 94.64%				

The features extracted using the DTCWT techniques have shown a better overall sensitivity when compared to the DWT techniques. The network is trained independently by 10,675 beats and tested over 93,894 beats which indicates that only 10% (approximate) of total data set is used for learning process. The remaining 90% of data is used for evaluating the performance of the classifier. In a confusion matrix the diagonal elements indicates the correctly classified beats corresponding to their respective classes. The feature set FS1 (DWT feature) classifies N , P, L, R and V beat with a sensitivity of 95.95%, 92.88%, 76.24%, 68.47% and 80.34% respectively. In clinical diagnosis, PVC beat has higher risk of sudden death compared to all other beats used in our experimental study [24]. Therefore it is important to classify V beats accurately. The feature set FS2 (DTCWT feature) classifies N , P, L, R and V beat with a sensitivity of 98.07%, 97.79%, 80.65%, 82.26% and 84.25% respectively. A comparative study on these feature set also indicates that the DTCWT technique outperforms the DWT technique. The overall sensitivity for feature set FS1 and FS2 are given by 91.23% and 94.64% respectively which indicates that the aforementioned feature extraction technique can be used as an excellent model for detecting cardiac arrhythmias. The Table 3.6 indicates the recent works on ECG beats detection using the MIT-BIH database. In [30], four different ECG beats were classified using Lyapunov exponents, wavelet coefficients and the power levels of power spectral density (PSD) as feature and MLP neural network as a classifier. However, the experimental results were limited to a small data set. Hu,*etal.* have developed a heartbeat classification method by combining two classifier (local and global classifier) using mixture of experts and this technique achieved an accuracy of 94.0% for distinguishing the two class using mixture of expert classifier. In [29], the authors have used morphological and temporal features as feature set and linear discriminant for classifying ECG arrhythmia and achieved an accuracy of 85.9%.

Table 3.6: Recent works on automatic detection of ECG beats using the MIT-BIH database

Literature	Features	Classifier	Classes	Accuracy (%)
Chazal *et al.* [29]	Morphology and heartbeat interval	Linear discriminant	5	85.9
E.D.ubeyli [30]	Lyapunov exponents and wavelet coefficients	ANN Classifier	4	93.9
Hu *et al.* [37]	Time domain features	Mixture of Experts	2	94
Proposed method (FS1)	DTCWT and morphological features	ANN Classifier	5	94.64

3.5 Conclusion

The MLP based neural network was used for classifying ECG beats into 5 classes. The two sets of features extracted using DWT and DTCWT were independently classified by the MLP network. The experimental results indicate that the DTCWT based features perform better than the DWT technique and shows the highest detection accuracy of 94.64%. Hence this technique can be used as a diagnostic tool to aid the physicians in determining the cardiac arrhythmias.

CHAPTER 4

CONCLUSIONS

4.1 Conclusion

In this work we have explored the ability of dual tree complex wavelet transform in the classification of cardiac arrhythmias. The multi-resolution capability of wavelet transform makes the transform more suitable in pattern recognition problems. Though the conventional DWT provides good time frequency localization of a signal but the transform is shift variant because of the down sampling operation in each stage. This drawback can be overcomed by using DTCWT technique. The analytic representation of the filter banks of DWT gives DTCWT. The transform provides approximate shift invariance with a limited redundancy of 2:1 for 1D signals. The transform decomposes the input signal into real and imaginary components and compute the magnitude information which helps in localizing the energy of wavelet basis functions. The analytic representation of signal gives a non-negative spectrum in the Fourier domain resulting in reduced bandwidth requirement and thereby overcoming the problem of aliasing which occurs among the frequencies of filter banks leading to perfect reconstruction. In addition to the features obtained after DWT and DTCWT transformation, four other features (AC power, kurtosis, skewness and RR interval ratio) extracted from QRS complex of each cardiac cycle is concatenated with the features obtained using DWT and DTCWT technique. Two methodologies are used to extract the features using DWT and DTCWT technique. The DTCWT technique extracts features from detail coefficients of 4th and 5th scale decomposition while the DWT technique extracts features from statistical parameters of six sub bands (D1-D5 & A5). Total two sets of features are extracted using the above mentioned techniques. These features were independently classified using MLP-NN which employs a back propagation algorithm with adaptive learning rate. The experimental result shows that the features extracted using the DTCWT technique shows a better performance when compared to the DWT technique. The experimental study is performed on 48 files of MIT-BIH arrhythmia database and has shown the highest promising sensitivity of 94.64% which indicates that this technique is an excellent model for computer aided diagnosis of cardiac arrhythmias.

4.2 Future works

The major objective of this project is to implement an algorithm which can classify diseased ECG beats. The experimental results using DTCWT technique has given satisfactory performance but still some additional works could be done in future such as :-

(i) The experimental study is performed using MLP-NN classifier. The optimization of synaptic weights and hidden nodes may give a better classification performance when compared to the performance of existing MLP network.

(ii) The experimental study can be extended to other classifier models such as support vector machines, Gaussian mixture models and a comparative study can be performed on their performance with MLP network.

(iii) The experimental study can be extended to a larger number of classes.

(iv) The R-peak locations in the experiment are taken from the annotation file of MIT-BIH database. An automatic R-peak detection algorithm needs to be implemented which can detect the R peak locations of ECG signals.

PUBLICATIONS

M. Thomas, M.K. Das, and S. Ari, “Classification of Cardiac Arrhythmias based on Dual Tree Complex Wavelet Transform,” in *proceedings of IEEE International* Conference *on Communication and Signal Processing-ICCSP 2014.*

BIBLIOGRAPHY

[1].R. U. Acharya, J. S. Suri, J. A. E. Spaan, and S. M. Krishnan, “Advances in Cardiac Signal Processing”. Springer, 2007.

[2]. W. J. Germann and C. L. Standield, “Principles of Human Physiology,” Benjamin Cummings, San Francisco, 2002.

[3]. John P. Fisher,“Heart: Cardiac Function & ECGs”, Textbook Of Medical Physiology, 11th edition 2012.

[4]. Lippincott Williams & Wilkins, “ECG Interpretation made incredibly easy”, 5th edition 2011.

[5]. Available online: http://www.nottingham.ac.uk/nursing/practice/resources/cardiology/function/bipolar_leads.php

[6]. Available online: http://www.eetimes.com/document.asp?doc_id=1278714

[7].Available online: http://en.wikipedia.org/wiki/Electrocardiography#Waves_and_intervals

[8]. X. Hu, Z. Xiao, N. Zhang, “ Removal of baseline wander from ECG signal based on a statistical weighted moving average filter”, *Journal of Zhejiang University-SCIENCE C (Computers & Electronics),* vol 12, pp. 397-403, 2011

[9]. G.M. Friesen, T.C. Jannett, M.A. Jadallah, S.L. Yates, S.R. Quint, and H.T. Nagle, “A comparison of the noise sensitivity of nine QRS detection algorithm,” *IEEE Trans. Biomed. Eng*. Vol. 37, pp. 85–98, 1990.

[10]. MIT-BIH Database distribution. http://www.physionet.org/physiobank/database/mitdb/

[11]. D.L. Fugal, “Conceptual wavelets in digital signal processing,” *Space and Signal Technologies,* 2009

[12]. S. C. Saxena, V. Kumar, and S. Hamde. Feature extraction from ECG signals using wavelet transform for disease diagnostics. IJSS, 33:1073– 1085, 2002.

[13]. Daubechies, “Where do wavelets come from? a personal point of view,” *Proceedings of the IEEE,* vol. 84, no. 4, pp. 510-513, Apr. 1996.

[14]. C. S. Burrus, R. A. Gopinath, and H. Guo, *Introduction to wavelets and wavelet transforms, a primer*. Prentice Hall, 1998.

[15]. S. C. Pei and P. W. Wang, "Discrete inverse transform with least square error in time-frequency filters," *IEEE Trans. Signal Process*., vol. 58, no. 7, pp. 3557 - 3568, Jul. 2010.

[16].P.D. Shukla, "Complex wavelet transform and their application," Thesis submitted for the degree of M.phil at University of Strathclyde, UK, Oct 2003

[17].N.Kingsbury, "Complex wavelets for shift invariant analysis and filtering of signal," *Applied and Computational Harmonic Analysis,*no.10, pp. 234-253, 2010.

[18]. Y. Özbay, "A new approach to detection of ECG Arrhythmias: Complex Discrete Wavelet Transform based Complex Valued Artificial Neural Network", *Springer Science - J Med Syst*em, vol.33, pp. 435-445, Sep 2008

[19]. Sathesh, S. Manoharan, "A Dual tree complex wavelet transform construction and its application to image denoising," *International Journal of Image Processing(IJIP),* vol 3.

[20]. S. Karpagachelvi, M. Arthanari, M. Sivakumar, "Classification of ECG signals using extreme learning machine," *Computer and Information Science,* vol 4, no. 1, Jan 2011.

[21]. A. Singer, "Wavelet transforms and adaptive Neuro-fuzzy inference system for color texture classification," *Expert systems and Applications,* vol. 34, pp. 2120-2128, 2008.

[22]. O.T. Inan, L. Giovangrandi and G.T. Kovacs, "Robust neural network based classification of premature ventricular contraction using wavelet transform and timing interval feature," *IEEE Transactions on Biomedical Engineering,* vol 53, no.12, Dec 2006.

[23]. M. Korurek, and B. Dogan, " ECG beat classification using particle swarm optimization and radial basis function neural network," *ExpertSystems with Applications*, vol. 37, pp. 7563-7569, 2010.

[24]. S.N. Yu and Y.H. Chen, "Electrocardiogram beat classification based on wavelet transformation and probabilistic neural network," *Pattern Recognition*, vol 28, pp.1142-1150, 2007.

[25]. Y.H. Chen, S.N Yu, “Selection of effective features for ECG beat recognition based on nonlinear correlations,” *Artificial Intelligence in Medicine,* vol54, pp.43– 52, 2012

[26]. R.J. Marti’s, U.R. Acharya, A.K. Ray, “Application of principle component analysis to ECG signals for automated diagnosis of cardiac health,” *Expert system with applications*, vol 39, pp.11792-11800, 2012.

[27]. G. Chen, “Automatic EEG seizure detection using dual-tree complex wavelet-Fourier feaftures,” *Expert system with applications*, vol 41, pp.2391-2394, Apr 2014.

[28]. K. Polat, and S. Guines, “Detection of ECG Arrhythmia using a differential expert system approach based on principal componentanalysis and least square support vector machine,” *Applied Mathematicsand Computation*, vol. 186, pp. 898-906, 2007.

[29]. P.D. Chazal, M.O. Dwyer, R.B. Reilly, “Automatic classification of heartbeats Using ECG morphology and heartbeat interval features,” *IEEE Transactions on Biomedical Engineering*, vol 51, no.7, Jul 2004.

[30]. E. D. Übeyli, “Statistics over features of ECG signals,” *Expert Systems with Applications*, vol 36, pp. 8758–8767, 2009.

[31]. D. Cvetkovic, E. Derya, I. Cosic, “Wavelet transform feature extraction from human PPG, ECG and EEG signal responses to ELF PEMF exposures: A pilot study,” *Digital signal processing*, vol 18, no.5, pp.867-874, Sep 2008.

[32]. K.P. Lil and W.H. Chang, “QRS Feature Extraction Using Linear Prediction,” *IEEE Trans. Biomed. Eng.* vol. 36, no. 10, 1989.

[33]. N.M. Arzeno, Z. Deng and C.S. Poon, “Analysis of First –Derivative base QRS detection algorithms,” *IEEE Trans. Biomed. Eng.*, vol. 55, pp. 478–484, 2008.

[34]. J. Pan, W. J. Tompkins, “A real time QRS detection algorithm,” *IEEE Trans. Biomed. Eng.*, vol. 32, pp. 230– 236, 1985.

[35]. Y.C. Yeha, and W. J. Wang, “QRS complexes detection for ECG signals The Difference Operation Method (DOM),” Computer *methods and programs in biomedicine,* vol. 9, pp. 245–254, 2008.

[36]. C. Li, C. Zheng, and C.Tai, “Detection of ECG characteristic points using Wavelet Transforms,”*IEEE Trans.Biomed. Eng, vol*. 42, no. 1, Jan 1995

[37]. Y.H. Hu, S. Palreddy, W.J. Tompkins, “A patient adaptable ECG beat classifier using a mixture of experts approach,” *IEEE Transactions on Biomedical Engineering*, vol 44, no.9, Sep 1997.

[38]. M. Javadia, S. Ali, A. A. Aranib, A. Sajedina, and R. Ebrahimpourb, “Classification of ECG arrhythmia by a modular neural network based on Mixture of Experts and Negatively Correlated Learning,” *Biomedical Signal Processing and Control*, vol. 8, pp. 289-296, 2013.

[39]. S. Haykin, *Neural networks*, New Delhi: Pearson Education Asia, 2002.

[40]. R. Ceylan and Y. zbay, “Comparison of FCM, PCA and WT techniques for classification ECG arrhythmias using artificial neural network, *Expert Systems with Applications*, vol. 33, no. 2, pp. 286-295, Aug. 2007.

[41]. H.G Hosseini, K.J.Reynolds, D. Powers, “A multi-stage neural network classifier for ECG events”, *2001 Proceedings of the 23rd Annual EMBS International Conference,* Istanbul, Turkey, Oct 2001

[42]. T.Ince, S. Kiranyaz, and M. Gabbouj, “A generic and robust system for automated patient-specific classification of ECG signals,” *IEEE Trans. Biomed. Eng.* vol. 56, pp. 1415-1426, 2009.

[43]. S. Osowski and T. L. Linh, “ECG beat recognition using fuzzy hybrid neural network,” *IEEE Trans.Biomed. Eng.*, vol. 48, no. 11, pp.1265–1271, Nov. 2001.

[44]. X. Yao, “Evolving artificial neural networks,” *Proc. IEEE*, vol. 87, no. 9, pp. 1423–1447, Sep. 1999.